Thermoelectric and Structural Characterization of Al-Doped ZnO/Y$_2$O$_3$ Multilayers

P. Mele[1, *, †], S. Saini[2, *, †], A. Tiwari[2], P. E. Hopkins[3], K. Miyazaki[4], A. Ichinose[5],
J. Niemelä[6], and M. Karppinen[6]

[1] *Research Center for Environmentally Friendly Materials Engineering, Muroran Institute of Technology, 050-8585 Muroran, Japan*
[2] *Department of Materials Science and Engineering, University of Utah, 84112 Salt Lake City, Utah, USA*
[3] *Department of Mechanical and Aerospace Engineering, University of Virginia, 22904 Charlottesville, Virginia, USA*
[4] *Department of Mechanical Engineering, Kyushu Institute of Technology, 804-0015 Kitakyushu, Japan*
[5] *Electric Power Engineering Laboratory, Central Research Institute of Electric Power Industry (CRIEPI), 240-0101 Yokosuka, Japan*
[6] *Department of Chemistry, Aalto University, 00076 Espoo, Finland*

The influence of Y$_2$O$_3$ nanolayers on thermoelectric performance and structure of 2% Al-doped ZnO (AZO) thin films has been studied. Multilayers based on five 50 nm thick AZO layers alternated with few nanometers thick Y$_2$O$_3$ layers were prepared by pulsed laser deposition on Al$_2$O$_3$ single crystals by alternate ablation of AZO target and Y$_2$O$_3$ target. The number of laser shots on Y$_2$O$_3$ target was maintained very low (5, 10 and 15 pulses in three separate experiments. The main phase (AZO) presents polycrystalline orientation and typical columnar growth not affected by the presence of Y$_2$O$_3$ nanolayers. The multilayer with 15 laser shots of Y$_2$O$_3$ showed best thermoelectric performance with electrical conductivity $\sigma = 48$ S/cm and Seebeck coefficient S = -82 μV/K, which estimate power factor (S$^2 \cdot \sigma$) about 0.03×10^{-3} W m^{-1} K^{-2} at 600 K. The value of thermal conductivity (κ) was found 10.03 W m^{-1} K^{-1} at 300 K, which is one third of typical value previously reported for bulk AZO. The figure of merit, ZT = S$^2 \cdot \sigma \cdot$ T/κ, is calculated 9.6×10^{-4} at 600 K. These results demonstrated the feasibility of nanoengineered defects insertion for the depression of thermal conductivity.

Keywords: ZnO Multilayers, Thermal Conductivity, Phonon Scattering.

1. INTRODUCTION

ZnO is a *n*-type semiconductor[1] with versatile applications such as optical devices in ultraviolet region,[2] piezoelectric transducers,[3] transparent electrode for solar cells,[4] gas sensors.[5] Apart from it, bulk ZnO was recognized as good candidate for thermoelectric applications[6] due to its low-cost, nontoxicity, and stability over a wide range of temperature. Sintered ZnO was added with several kinds of dopants in order to improve its thermoelectric performance, expressed by adimensional figure of merit, ZT:

$$ZT = (\sigma S^2)T/\kappa \qquad (1)$$

Where S: Seebeck coefficient; σ: electrical conductivity; κ: total thermal conductivity T: absolute temperature.[7]

Review on bulk thermoelectric oxides can be found in Ref. [8]: extensive comparison with other *n*-type and *p*-type oxides reveals that ZnO (doped with Ga and Al) is currently the bulk oxide with the largest ZT = 0.65 at 1000 C.[9] ZT of nanostructured Bi$_2$Te$_3$/Sb$_2$Te$_3$ is superior with ZT = 2.4 at 300 K,[10] however is not sustainable due to the high cost (Te) or toxicity (Bi) of the constituent elements. On the other hand, ZT of ZnO surely requires an enhancement to be disclosed to practical applications. As suggested in 1993 by Hicks and Dresselhaus,[11, 12] one possible strategy to enhance ZT is the depression of κ through reduction of the phonon mean free path. The natural defects of the material (such as grain boundaries, dislocation, atomic defects, segregation of secondary phases, and so on) may act as phonon scatterers being on the nanometric scale. This kind of approach is general and can be applied to any category of material. However is apparent that, respects to bulk materials, thin films allow control

of the morphology and crystalline orientation at a superior level. This is how in the recent times the performance of high-quality and dense ZnO thin films prepared by a variety of techniques[13–33] was reported as quite high, with significantly low values of $\kappa = 2\sim6$ W/m K and high values of ZT = 0.016∼0.05 at room temperature, surpassing the performance of the corresponding bulk material.[13, 16–19] The highlight of this research are the RF sputtered AZO films (grain size 30 nm)[25] presenting $\kappa = 1.19$ W/m K and ZT > 0.1 at room temperature. These outstanding results have been realized thanks to the careful control of morphology and crystalline orientation of the films. Especially, the reduction of grain size to few tens of nanometers leads to enhanced phonon scattering due to enhanced number of grain boundaries and, at last, to low thermal conductivity and high ZT.

Furthermore, it is possible to incorporate in the thin films additional *artificial* nanodefects, increasing the concentration of the phonon scatterers, leading to further depression of κ. Several kinds of nanodefects can be introduced in the film, such as nanolayers, nanostructures, nanoprecipitates, or nanopores. In superconducting oxide thin films, impressive enhancement of the critical current have been obtained in the last ten years thanks to the control of distribution, size and morphology of the nanodefects. On the contrary, the nanoengineering approach has been seldom utilized in the case of thermoelectric oxide thin films. For example, outstanding results have been reported by Ohta et al.,[34] showing giant thermoelectric Seebeck coefficient (850 μV/K) of a two-dimensional electron gas in $SrTiO_3$/Nb-$SrTiO_3$ multilayers fabricated by pulsed laser deposition.

In this work, we describe the thermoelectric properties of AZO/Y_2O_3 multilayers prepared by PLD on sapphire. We will discuss the role of Y_2O_3 nanolayers in the depression of thermal conductivity and enhancement of ZT.

2. EXPERIMENTAL DETAILS

Multilayered films comprising of $Zn_{0.98}Al_{0.02}O$ (AZO) layers and Y_2O_3 layers were prepared by pulsed laser deposition (PLD) technique using a Nd:YAG laser (266 nm).

To prepare AZO/Y_2O_3 multilayers on Al_2O_3 (100) single crystals, Y_2O_3 target and AZO target were alternating ablated. The Y_2O_3 target was purchased (Toshima Ltd., Tokyo, Japan), while AZO target was prepared by spark plasma sintering (SPS) as described separately.[24] At first, very small numbers of laser pulses (5, 10 and 15 in three separate experiments) were shot on Y_2O_3 target at 800 °C with 200 m Torr of O_2 to generate Y_2O_3 islands on the Al_2O_3 bare substrate. Then, after deposition system is cooled down at room temperature under 400 Torr of O_2. To deposit the first AZO layer, temperature was raised up to 400 °C with 200 m Torr of O_2. Y_2O_3 islands were deposited on AZO layer in the same conditions used at

the beginning. Then, the second AZO layer deposition followed under same initial conditions, and so on. Designed configurations kept the lengths of AZO layers to 50 nm and total thickness of the multilayers to 500 nm (so that 5 AZO layers were fabricated). The thicknesses of the layers were controlled by number of pulses in PLD, after determination of growth rate of AZO on Al_2O_3 substrate. Total time required to prepare a multilayer was about 25 hours.

The targets were rotated during the irradiation of laser beam. The substrates were glued with silver paste on Inconel plate customized for ultrahigh vacuum applications. Deposition parameters such as laser energy (4.2 J/cm^2) pulse frequency (10 Hz), substrate-target distance (about 35 mm) and rotation speed of the target (25 rotations per minute) were kept unchanged during all the deposition routines.

The structural characterization was performed by X-ray diffraction (at wavelength of $CuK_{\alpha} = 1.54056$ Å) (XRD) (Bruker D8 Discover) and Grazing Angle X-ray diffraction (GIXRD) (PANanalytical X'Pert Pro MPD).

Morphology was checked by transmission electron microscopy (TEM; JEOL 2010F). The thickness and in-plane roughness were obtained by a Keyence VK-9700 3D microscope. Surface of Al_2O_3 substrates after deposition of Y_2O_3 islands was checked by scanning probe microscope (SPM 5500, Agilent Technologies). The electrical conductivity was measured from 300–600 K by a custom-built four-point-probe technique consisting of a current source (ADCMT 6144), a temperature controller (Cryo-con 32) and a nano voltmeter (Keithley 2182A). Seebeck coefficient were measured from 300–600 K with a commercially available system (MMR Technologies SB-100). The out-of-plane thermal conductivities of thin films at room temperature were measured with time domain thermoreflectance (TDTR).[25, 26]

3. RESULTS AND DISCUSSION

With the intention of inserting nanosized layers of Y_2O_3 between AZO layers, we shot on the Y_2O_3 target very limited number of laser shots (5, 10 and 15). The observation at AFM revealed the formation of Y_2O_3 islands, which concentration is proportional to number of pulses (Fig. 1). Figure 2 shows cross-sectional TEM image of the multilayers prepared with different amount of Y_2O_3 shots between the AZO layers. AZO grains grown with typical columnar shape reported for single layered AZO films on same substrate.[16–18] Y_2O_3 nanoislands cannot be identified between the AZO layers: instead, very thin layers (thickness about 2 nm) are visible in high magnification TEM images. SEM-EDS elementary analysis reveals deficiency of Zn and Al in correspondence to the nanolayers, but presence of Y element was not noticed. The formation of thin layers is due to the coarsening of the Y_2O_3 islands and, possibly, to reaction occurring between AZO and Y_2O_3 after the deposition of the second AZO layer.
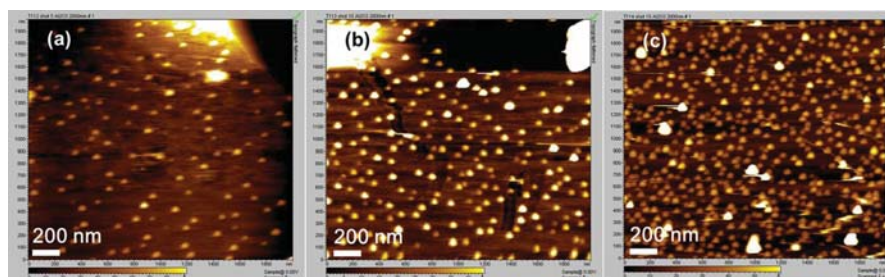
Figure 1. AFM images of the surface of AZO layer (2 μm^2 areas) after the deposition of Y$_2$O$_3$ islands on Al$_2$O$_3$ crystal: (a) 5 pulses (b) 10 pulses and (c) 15 pulses of laser on Y$_2$O$_3$ target.
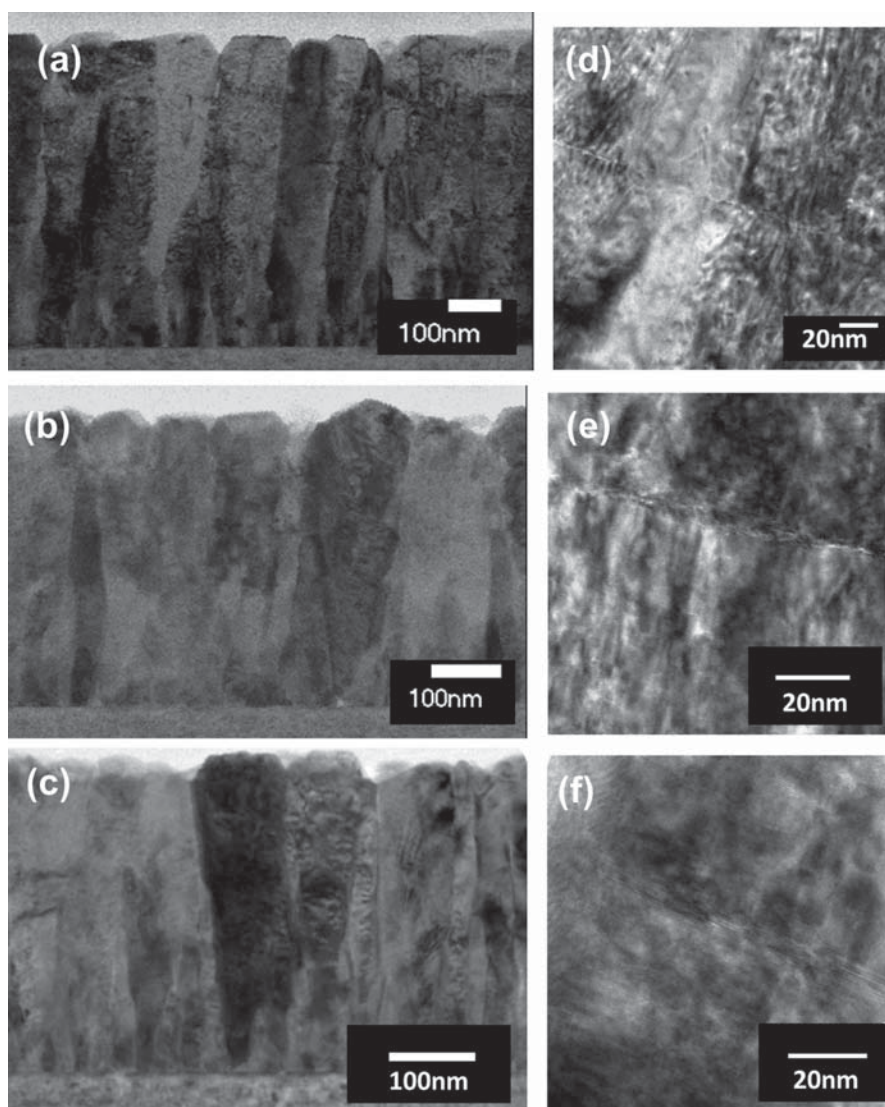

Figure 2. Cross-sectional TEM images of the AZO/Y$_2$O$_3$ multilayers. Left column: low magnification TEM of (a) AZO layers alternated with 5 pulses of Y$_2$O$_3$; (b) AZO layers alternated with 10 pulses of Y$_2$O$_3$; (c) AZO layers alternated with 15 pulses of Y$_2$O$_3$. Right column: high magnification of the interface between consecutive AZO layers: (d) AZO layers alternated with 5 pulses of Y$_2$O$_3$; (e) AZO layers alternated with 10 pulses of Y$_2$O$_3$; (f) AZO layers alternated with 15 pulses of Y$_2$O$_3$.
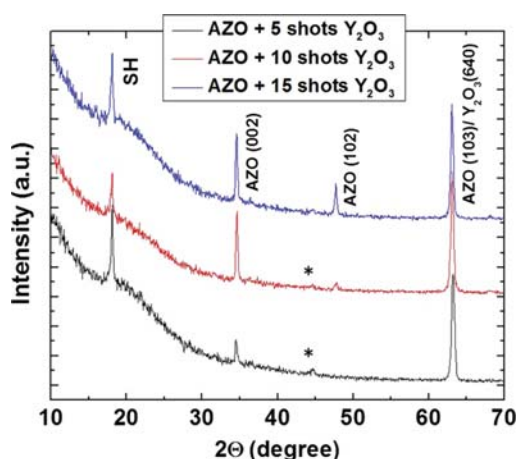
Figure 3. GIXRD patterns of AZO/Y$_2$O$_3$ multilayers. SH indicates a reflection from the sample holder. Asterisks denote unidentified peaks.

Figure 3 shows GIXRD pattern of AZO/Y$_2$O$_3$ multilayers deposited on single crystal Al$_2$O$_3$ at 400 °C. (002) peak of AZO appeared together with (102) and (103) reflections, so that preferential *c*-axis orientation (testified by the presence of (002) peak only) was not reached and the AZO layers are polycrystalline. In addition, since (103) reflection of AZO overlaps with (640) peak of Y$_2$O$_3$, it is not possible to confirm the presence of Y$_2$O$_3$ between the AZO layers. The rocking curves of AZO (002) peak (not reported here) show full widths at half maximum (FWHM) of about 4 degrees, sign of low crystallinity of the AZO phase. Unidentified peaks in the GIXRD pattern (marked with asterisks) may be attributed to the new phase which constitutes the thin layers. The presence of Y$_2$O$_3$ nano-sized interlayers is expected to affect the phonon scattering of these multilayers. Transport and thermoelectrical characterization is shown in Figure 4 in the range of 300 K to 600 K and reported in Table I. Electrical conductivity (Fig. 4(a)) is higher for the multilayers with 5 shots of Y$_2$O$_3$ for all temperature range, while the other two multilayers show lower and almost similar conductivity.

Overall, the values of σ are a third respect as we reported for ∼500 nm AZO single-layered films on Al$_2$O$_3$.[18] These results may be explained with the poor crystallinity of the multilayers in comparison with the single layers.

Figure 4(b) shows influence of Y$_2$O$_3$ shots on Seebeck coefficient. Due to Al^{3+} doping and oxygen vacancies, the multilayers show negative Seebeck coefficient.[6]

From the values of Seebeck coefficient and electrical conductivity, we have calculated the power factor (PF) of thin films as $PF = \sigma \cdot S^2$. Figure 5(a) shows the value of PF for multilayers added with different amounts of Y$_2$O$_3$ in the temperature range 300 K to 600 K. 10 shots and 15 shots–added multilayers present comparable values of PF in the whole range of temperature, while the 5-shots multilayer presents lower PF due to lower value of S. As expected, the samples with lower σ show the highest absolute value of S, as can be justified by phononic scattering due to impurities, point defects and grain boundaries.[12]

Further, we measured thermal conductivity of thin films using time domain thermo reflectance technique and reported in Table I. It is apparent that the small variation in the number of Y$_2$O$_3$ pulses is not dramatically affecting the value of κ, which is reduced of about a third respect to corresponding bulk materials, but increased as double respect to the single layered AZO/Al$_2$O$_3$ thin film,[18] against our assumptions. The thermal conductivity of a material is extremely dependent on quality, so slight changes in growth temperature or parameters that could lead to changes in material structure or defect levels will change the thermal conductivity. In general, this might be able to explain the various discrepancies in measured thermal conductivity. In particular, the AZO/Y$_2$O$_3$ multilayer system requires deeper investigation varying not only the growth parameters but also the ratio between the thicknesses of the layers to depict the complex scenario of the thermal conductivity behavior.

Dimensionless figure of merit ZT is calculated and reported in Table I. The behavior of ZT values for thin films at elevated temperatures are estimated using κ at 300 K ($\kappa_{300\ K}$) and shown in Figure 5(b).
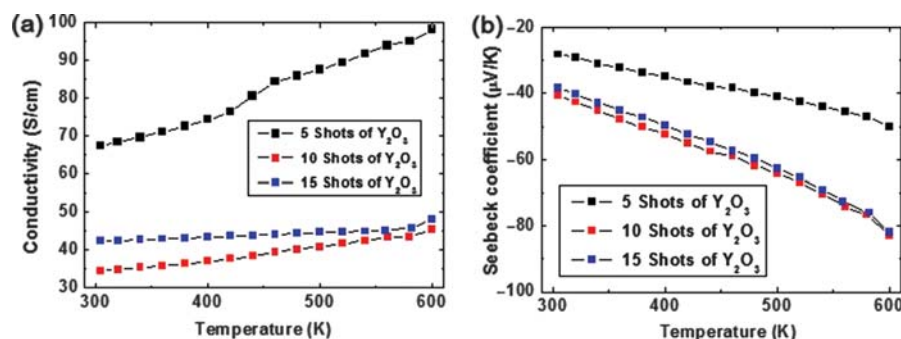

Figure 4. (a) Temperature dependence of the electrical conductivity and (b) Seebeck coefficient for the three multilayers in function of number of Y$_2$O$_3$ shots between AZO layers.

Table I.   Thermoelectric properties of AZO multilayers at 300 K/600 K.

Samples	Electrical conductivity σ (300 K/600 K)	Seebeck coefficient S (300 K/600 K)	Power factor PF (300 K/600 K)	Thermal conductivity k (300 K)	Error	ZT (300 K/600 K)	Reference
AZO-Y$_2$O$_3$ multilayers on Al$_2$O$_3$	S/cm	μV/K Wm^{-1}	10^{-3}Wm^{-1}K^{-2}	Wm^{-1}K^{-1}			
Number of Y$_2$O$_3$ pulses							
5	67/98	$-28/-50$	0.0054/0.0247	10.51	1.52	$1.5 \times 10^{-4}/7.0 \times 10^{-4}$	This work
10	34/45	$-40/-82$	0.0057/0.031	13.12	1.76	$1.3 \times 10^{-4}/7.1 \times 10^{-4}$	This work
15	42/48	$-38/-82$	0.006/0.03	10.03	1.19	$1.8 \times 10^{-4}/9.6 \times 10^{-4}$	This work
Single AZO layer on Al$_2$O$_3$	299/291	$-58/-126$	0.1/0.43	6.897		0.004/0.036	[18]
AZO bulk	206/152	$-132/-150$	0.35/0.34	34		0.0034/0.014	[18]
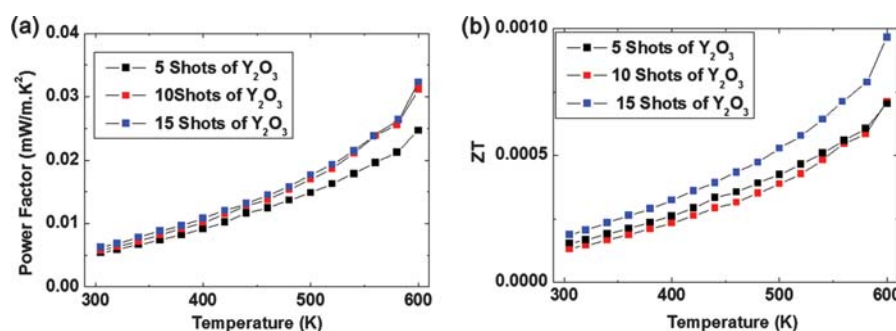
Figure 5. Thermoelectric performance: (a) power factor (PF) versus temperature; (b) dimensionless figure of merit ZT at elevated temperatures using thermal conductivity at 300 K for AZO multilayers added with different amounts of Y$_2$O$_3$.

This approach is used on the basis of the following facts:

(i) in columnar films of ZnO whose morphology is quite similar to ours, in plane thermal conductivity values determined in different conditions are always higher than out of plane values[26] and

(ii) the thermal conductivity of ZnO films is found to decrease with increasing temperature.[32]

15-shots AZO multilayer shows best ZT value 0.0001 among all multilayers at 300 K and predicted enhancement up to 0.001 at 600 K.

4. CONCLUSION

In this contribution, we studied the feasibility to add artificial defects on the nanoscale to depress thermal conductivity of AZO thin films through enhanced phonon scattering. We tried to insert tiny Y$_2$O$_3$ nanolayers in 500 nm AZO films. We obtained encouraging result since the value of thermal conductivity was lower respect to the case of bulk material: 10.03 W m^{-1} K^{-1} for AZO/Y$_2$O$_3$ multilayers and 34 W m^{-1} K^{-1} for bulk AZO. However, the reduction of κ is less significant than in single layered AZO films deposited on the same substrate and in comparable conditions. Furthermore, the transport properties of the multilayers appear worse than for the typical AZO thin films. We attribute this to the poor crystallinity of the multilayers if compared with the crystallinity of the single layers.

We expect more significant depression of thermal conductivity through modification of the deposition conditions to enhance AZO crystallinity and control of the Y$_2$O$_3$ layers thickness.

References and Notes

1. U. Ozgür, Ya. I. Alivov, C. Liu, A. Teke, M. A. Reschikov, S. Dögan, V. Avrutin, S.-J. Cho, and H. Morko, *J. Appl. Phys.* 98, 041301 (**2005**).
2. G. M. Ali and P. Chakrabarti, *J. Phys. D: Appl. Phys.* 43, 415103 (**2010**).
3. P. X. Gao and Z. L. Wang, *J. Appl. Phys.* 97, 044304 (**2005**).
4. M. Law, L. E. Greene, J. C. Johnson, R. Saykally, and P. Yang, *Nat. Mater.* 4, 455 (**2005**).
5. M. Kaur, S. V. S. Chauhan, S. Sinha, M. Bharti, R. Mohan, S. K. Gupta, and J. V. Yakhmi, *J. Nanosci. Nanotech.* 9, 5293 (**2009**).
6. M. Ohtaki, T. Tsubota, K. Eguchi, and H. Arai, *J. Appl. Phys.* 79, 1816 (**1996**).

7. H. Böttner, *Mater. Res. Soc. Symp. Proc.* 1166 (**2009**); J. P. Wiff, Y. Kinemuchi, and K. Watari, *Mater. Lett.* 63, 2470 (**2009**).

8. J. W. Fergus, *Journal of the European Ceramic Society* 32, 525 (**2012**).

9. M. Ohtaki, K. Araki, and K. Yamamoto, *J. Electr. Mater.* 38, 1234 (**2009**).

10. R. Venkatasubramanian, E. Siivola, T. Colpitts, and B. O'Quinn, *Nature* 413, 517 (**2001**).

11. L. D. Hicks and M. S. Dresselhaus, *Phys. Rev. B* 47, 16631 (**1993**).

12. L. D. Hicks and M. S. Dresselhaus, *Phys. Rev. B* 47, 12727 (**1993**).

13. P. Mele, Nanostructured thin films of thermoelectric oxides, Oxide Thin Films, Multilayers and Heterostructures, edited by P. Mele, T. Endo, S. Arisawa, C. Li, T. Tsuchiya, Springer, Switzerland (**2015**), Chap. 8.

14. Y. Inoue, M. Okamoto, T. Kawahara, Y. Okamoto, and J. Morimoto, *Mat. Trans.* 46, 1470 (**2005**).

15. A. I. Abutaha, S. R. Sarath Kumar, and H. N. Alshareef, *Appl. Phys. Lett.* 102, 053507 (**2013**).

16. P. Mele, S. Saini, H. Honda, K. Matsumoto, K. Miyazaki, H. Hagino, and A. Ichinose, *Appl. Phys. Lett.* 102, 253903 (**2013**).

17. S. Saini, P. Mele, H. Honda, D. J. Henry, P. E. Hopkins, L. Molina-Luna, K. Matsumoto, K. Miyazaki, and A. Ichinose, *Japan. J. Appl. Phys.* 53, 060306 (**2014**).

18. S. Saini, P. Mele, H. Honda, T. Suzuki, K. Matsumoto, K. Miyazaki, A. Ichinose, L. Molina Luna, R. Carlini, and A. Tiwari, *Thin Solid Films* 605, 289 (**2016**).

19. N. Vogel-Schauble, T. Jaeger, Y. E. Romanyuk, S. Populoh, C. Mix, G. Jakob, and A. Weidenkaff, *Phys. Status Solidi RRL* 7, 364 (**2013**); and Erratum, *ibid., Phys. Status Solidi RRL* 8, 206 (**2014**).

20. N. Vogel-Schauble, Y. E. Romanyuk, S. Yoon, K. J. Saji, S. Popuolh, S. Pokrant, M. H Aguirre, and A. Wiedenkaff, *Thin Sol. Films* 520, 6869 (**2012**).

21. F. Gather, A. Kronenberger, D. Hartung, M. Becker, A. Polity, P. J. Klar, and B. K. Meyer, *Appl. Phys. Lett.* 103, 082115 (**2013**).

22. H. Liu, L. Fang, D. Tian, F. Wu, and W. Li, *J. Alloys and Comp.* 588, 370 (**2014**).

23. S. Teehan, H. Efstathiadis, and P. Haldar, *J. Alloys and Comp.* 509, 1094 (**2011**).

24. H. Hiramatsu, W.-S. Seo, and K. Koumoto, *Chem. Mater.* 10, 23033 (**1998**).

25. J. Loureiro, N. Neves, R. Barros, T. Mateus, R. Santos, S. Filonovich, S. Reparaz, C. M. Sotomayor-Torres, F. Wyczisk, L. Divay, R. Martins, and I. Ferreira, *J. Mater. Chem. A* 2, 6649 (**2014**).

26. Y. Xu, M. Goto, R. Kato, Y. Tanaka, and Y. Kagawa, *J. Appl. Phys.* 111, 084320 (**2012**).

27. A. El Amrani, F. Hijazi, B. Lucas, J. Boucle, and M. Aldissi, *Thin Solid Films* 518, 4582 (**2010**).

28. J.-S. Tian, M.-H. Liang, y.-T. Ho, Y.-A. Liu, and L. Chang, *J. Cryst. Growth* 310, 777 (**2008**).

29. T, Tynell, I. Terasaki, H. Yamauchi, and M. Karppinen, *J. Mater. Chem. A* 1, 13619 (**2013**).

30. T. Tynell, A. Giri, J. Gaskins, P. E. Hopkins, P. Mele, K. Miyazaki, and M. Karppinen, *J. Mater. Chem A* 2, 12150 (**2014**).

31. M. Ruoho, V. Plae, M.Erdmanis, and I. Tittonen, *Appl. Phys. Lett.* 103, 203903 (**2013**).

32. J. Alvarez-Quintana, E. Martinez, E. Perez-Tijerina, S. A. Perez-Garcia, and J. Rodriguez-Vejo, *J. Appl. Phys.* 107, 063713 (**2010**).

33. B. J. Lokhande, P. S. Patil, and M. D. Uplane, *Mat. Lett.* 57, 573 (**2002**).

34. H. Ohta, S. W. Kim, Y. Mune, T. Mizoguchi, K. Nomura, S. Ohta, T. Nomura, Y. Nakanishi, Y. Ikuhara, M. Hirano, H. Hosono, and K. Koumoto, *Nat. Mater.* 6, 129 (**2007**).